15A.5

IN SITU ICING VERIFICATION

David J. Smalley, Earle R. Williams, Michael F. Donovan
Robert G. Hallowell, Kenta T. Hood, Betty J. Bennett
MIT Lincoln Laboratory

Mengistu Wolde, Matthew Bastian
National Research Council of Canada

Alexei Korolev
Environment Canada

1. INTRODUCTION

The dual polarization (hereafter, dual pol) upgrade for the CONUS portion of the United States' NEXRAD network has been completed in 2013. The primary, functional upgrade is the ability to significantly improve estimates of the type of bulk scatterers contributing to the radar returns. The NEXRAD upgrade is delivered with a hydrometeor classification algorithm (Park *et al*., 2009) yielding ten categories. The Federal Aviation Administration (FAA) supports MIT Lincoln Laboratory (LL) to develop NEXRAD-based algorithms for their aviation weather systems focused on deriving benefit from the dual pol upgrade. By utilizing the hydrometeor classifications and dual pol data, new capabilities such as improving data quality and detecting potential icing hazards are possible.

The new capabilities are possible provided the underlying hydrometeor classifications and dual pol data are of high fidelity. With radar data volumes available as frequently as a bit over every four minutes, icing detection by radar adds a temporal and spatial resolution advantage to complement current methods used for aviation. In situ icing verification is the reference standard regarding the fidelity of radar-derived icing information. Pilot reports (PIREPs) of icing are available but have inherent uncertainty and limited sampling (Bernstein *et al*., 2007). The FAA NEXRAD Program Office is sponsoring a partnership between LL and the National Research Council of Canada (NRC) for the in situ verification and validation of hydrometeors and identification of potential icing hazards. Four, directed icing missions were executed within the radar range of dual pol NEXRADs (Cleveland and Buffalo) during February 2012 and 2013. The NRC's Convair 580 is fully equipped for icing missions with a full suite of thermodynamic, cloud microphysical, particle imaging, and on-board radar (W-band and X-band) sensors. Data from these sensors are used to determine the fidelity of the NEXRAD dual pol data and hydrometeor classifications.

A variety of winter weather events were encountered during more than 10 hours of direct measurements including fully glaciated clouds with various ice crystal types, mixed phase, and clear icing conditions. This paper will discuss the coordination of the icing missions, the discoveries during the missions, and recommendations regarding further development and improvement

----

Corresponding Author: David J. Smalley, MIT Lincoln Laboratory, 244 Wood Street, Lexington, MA 02420
e-mail: daves@ll.mit.edu

This work was sponsored by the Federal Aviation Administration (FAA) under Air Force Contract FA8721-05-C-0002. Opinions, interpretations, conclusions, and recommendations are those of the author and are not necessarily endorsed by the United States Government.

of NEXRAD hydrometeor classification and icing hazard algorithms.

2. MICROPHYSICS SUMMARY OF CRYSTAL TYPES

The dual pol radar returns and subsequent derivation of hydrometeor classifications relate to the microphysical conditions generating the bulk scatterers. For the concern of NEXRAD-based potential icing hazards identification, the fundamental challenge is the interpretation of the juxtaposition of returns from ice crystals, aggregates thereof, supercooled water drops (detectable) and droplets (inferred), and a mixture of all of the above. Dual pol data such as differential reflectivity and the correlation coefficient show responses to the different water species. The NEXRAD hydrometeor classifier algorithm (HCA) utilizes those data in part to generate its categories.

Williams *et al*. (2011) provides an in-depth exploration of the topic. A summary is appropriate here. Microphysics is the key. Essentially, at or above ice saturation the combination of temperature (at or below freezing) with the state of liquid water saturation dictates crystal types with or without the presence of supercooled liquid water. Figure 1 from Bailey and Hallett (2009) shows images of crystal types grown in laboratory diffusion chambers under controlled temperature and humidity. The arcing red curve in the figure shows the water saturation boundary with subsaturated conditions to the left and supersaturated to the right. Clearly there are crystal habit changes in response to the water saturation state. Similar results are found in nature.

Figure 2 summarizes in broad strokes the crystal types observed (such as in Figure 1). The water supersaturated conditions are above the dark curve with subsaturation below. Dual pol returns will differ depending on the dominant state of needles, plates, or dendrites that in turn also impact the likelihood of aggregation and further affect the dual pol returns. Further, if enough advection of water vapor is sustained, the Bergeron process can be maintained resulting in the dual presence of crystals (especially dendrites) and supercooled water. This is especially the case at temperatures around -10° C to -15° C. Korolev and Mazin (2003) present calculations relating sustainment of lift to supersaturation states highlighting the importance of quantifying vertical velocity.

Depending on the microphysics (and precipitation physics), a wide range of dual pol returns are possible which the hydrometeor classification algorithm needs to handle. Differential reflectivity (ZDR) ranges from slight negative for conical graupel to nearing +10 dB for large, flat aggregates. Wolde and Vali (2001a) recorded +6 to +7 dB ZDR for a mixture of plates and sector plates with +1 to +2 dB on dendritic crystals from airplane-based W-band radar polarimetric measurements verified by in situ particle imaging probes. The combination of ice and water saturation states in the context of temperature and sustainment of lift factor into the radar observables available to hydrometeor classification and icing hazard potential algorithms.

3. FUNDAMENTAL ASPECTS OF THE NEXRAD HYDROMETEOR CLASSIFICATION ALGORITHM

The NEXRAD Hydrometeor Classification Algorithm (Park *et al*., 2009), known as HCA, uses data from the radar moments and dual pol parameters in a fuzzy logic system to determine hydrometeor categories. Figure 3 lists the possible HCA categories on the left. Eight precipitation classifications are available: dry snow (DS), wet snow (WS), ice crystals (IC), big drops (BD), light/moderate rain (RA), heavy rain (HR), graupel (GR), and rain/hail mix (HA). Two data quality categories are provided for ground clutter (GC) and biological such as insects (BI). If HCA cannot determine a class despite viable data, the unknown (UK) class is reported. No data (ND) is representative of data below signal to noise thresholds. It is important to note that only one HCA classification per pulse resolution volume is permitted.

HCA also relies on the NEXRAD Melting Layer Detection Algorithm (MLDA) when brokering classifications. Like HCA, the MLDA uses data from the radar moments and dual pol parameters to yield a *single* melting layer. If necessary, the MLDA augments radar data with a meteorological model grid point sounding associated to the radar location to best determine the single melting layer. Beginning in the Spring of 2014, an option will be available to use a grid of model soundings over the radar coverage domain in lieu of the solitary grid point (Hallowell *et al*., 2013). It has been demonstrated that the grid method supports MLDA properly capturing with higher fidelity transitional melting levels within a radar domain (e.g. – frontal passages).

Classifications from HCA are constrained based on this single melting layer. Figure 3 lists the classes possible with respect to being mostly within, partly above or below, or mostly above or below the melting layer. Importantly, BD, RA, and HR classifications are not currently possible in below freezing conditions. Liquid water at a couple of degrees below freezing temperatures is the very supercooled water that could pose an icing potential. It may be challenging to modify HCA to at least partially allow for some liquid water classification at below freezing temperatures. The direct dual pol data might, too, be vague in this regard. In situ measurements to precisely identify such areas could be beneficial to this issue.

One classification – graupel - provides an inference for the presence of supercooled water. Graupel by definition is snow rimed by supercooled water (primarily ice crystals, less likely aggregates). It could occur in a mixed phase region or it could occur when snow formed aloft falls into a mixed phase or pure supercooled water region below. As reported by HCA, it can be interpreted that an icing potential is within and/or somewhat above the reported altitude.

With the NEXRAD network now dual pol, a broader assessment of HCA should be made. Certainly, an ability of MLDA and HCA to handle multiple freezing levels should be considered a priority. Any regional or seasonal issues that become evident should be addressed. Is a supercooled classification possible? Is a mixed phase classification possible? Are refinements to current classes warranted?

4. NEXRAD ICING HAZARD LEVELS ALGORITHM

MIT Lincoln Laboratory (LL) developed an Icing Hazard Levels (IHL) algorithm that will provide FAA aviation weather systems with an icing potential product based on analysis of NEXRAD dual pol data from single radars. Hallowell *et al*. (2013) details the development of the initial version of the product. In situ icing missions that provide verification of icing presence and hydrometeor types will directly benefit further truthing and planned development of IHL.

The IHL development cycle is incremental. New techniques for dual pol based icing hazard potential will be added as warranted to increase the IHL product's capability. The dual pol data are useful to rule in or rule out the possibility of an icing hazard. Not all icing hazard conditions will be detectable by NEXRAD's S-band dual pol monitoring. One benefit from the in situ icing missions will be to define the bounds of NEXRAD's capability. One benefit from IHL is that it provides a product for icing hazard potential via radar as frequently as a bit more than every 4 minutes. This should complement other icing potential determination methods.

Figure 4 illustrates the initial version IHL product that will be part of the NEXRAD baseline in 2014. It is compared against the Current Icing Potential product available from the Aviation Data Dissemination Service and PIREP reports of icing. IHL requires the presence of the graupel HCA class to determine top and bottom altitudes of an icing hazard potential based on the radar volume scanning strategy employed. When graupel is present, IHL augments the altitude determination by using temperature (T) and relative humidity (RH) analysis functions utilized as part of the National Center for Atmospheric Research's

Current Icing Potential product (Bernstein *et al*., 2005). The radar is not a thermometer so the T and RH vertical profiles are available to IHL from the RAP13 meteorological model. The fidelity of the IHL product then is related to the appropriateness of the HCA graupel classification and to the fidelity of the RAP13 model data. The former can be studied with in situ icing missions. From the radar and algorithmic consideration, when is snow (essentially crystals) rimed sufficiently for it to be considered graupel and then prevalent enough to become the singular choice from HCA?

The example in Figure 4 is from the Upton, NY NEXRAD (KOKX) for about 10 UTC on Feb. 24, 2012. Note the good agreement between IHL, CIP, and the PIREP. The PIREP altitude occurs between the altitude bounds from IHL. CIP utilizes non-dual pol NEXRAD data and PIREPs as part of its data input suite. Uncertainty bounds are associated with the PIREPs for many reasons (Bernstein *et al*., 2005, 2007). The CIP coverage for the New York area is more extensive than IHL. This is to be expected with the first version as the focus is on graupel inferred from radar. Future improvements for IHL are being explored to add a freezing drizzle aloft and/or mixed phase identification component. In situ icing missions will be extremely pertinent to the improvement effort.

In winter weather conditions, a few dual pol radar features are evident repeatedly. In Williams *et al*. (2011), two such features were dubbed Category A and Category B. Category A is a suspect area of icing potential possibly associated with mixed phase conditions. It is observed as a relative increase in positive ZDR at altitudes with temperature in the -10° C to -15° C range. Recall from Figures 1 and 2 that this region is favored for crystal generation. Category B is sometimes referred to as the cocoon – the trailing edges and cap to the weather where it is suspected that primarily crystals persist.

Figure 5 is a schematic of a radar PPI (plan position indicator) with five zones designated for their icing hazard potential. Zone 1 covers altitudes beneath the primary melting layer (as discovered top down from higher altitudes). This area is prone to additional freezing level crossovers. The thickness and number of alternating “warm” and “cold” layers will dictate the potential for additional icing potential. Finding evidence of icing in this lower altitude region is important to aviation due to lack of evasive options. At farther ranges from the radar location, this zone is below NEXRAD radar scans. For that, a mechanism to handle transition of the last known hydrometeors from higher up is an important goal. Zone 2 within the melting layer is where any combination of solid, liquid, and all variants in transition thereof can exist and pose a threat. Zone 3 is addressed (at least in part) by the IHL focus on graupel augmented with CIP T and RH constructs. Zone 4 is the Category A situation of the positive ZDR “bright band”. Zone 5 is the edge circumstance of Category B. A more complete IHL ideally accounts for these zones. One objective of the in situ icing missions is to target these zones.

5. IN SITU ICING MISSIONS

Ground observations are used where possible to verify or validate the appropriateness of hydrometeor classifications and IHL when lacking in situ icing missions. Smalley *et al*. (2011) describes findings from the partnership of LL and Valparaiso University for such observations in northern Indiana supplemented by local, on-demand atmospheric soundings collocated with a C-band dual pol radar. The incipient concepts behind signatures of Category A and B began with this effort prior to the NEXRAD dual pol upgrade. Similar ground observations are made in the eastern Massachusetts region without the benefit of soundings and removed 45 – 95 km from the nearest dual pol NEXRAD in Taunton, MA (KBOX). Figure 6 shows a mixed collection of hydrometeors from eastern Massachusetts during a winter storm in 2013. Rimed crystals and their fragments are evident along with ball-like graupel. PIREPs and IHL indicated spotty icing at times. While of value, collections of this sort are lacking the definition provided by in situ icing missions.

5.1 Flight Planning

The FAA NEXRAD Program Office is sponsoring a partnership between LL and NRC for the in situ verification and validation of hydrometeors and identification of potential icing hazards. Icing missions have been executed in the Lake Erie and Lake Ontario regions. From Bernstein *et al*. (2007), this is a prime region for both icing potential and supercooled large drop (SLD) icing potential. The single mission in February 2012 demonstrated the value of in situ measurements for validation of hydrometeor classification. The icing mission was focused over Lake Erie probing a Category B (edge) event. In February 2013, three missions were executed primarily south of Lake Ontario. In all cases, NEXRAD dual pol returns were used in real-time to direct probing. Preliminary findings from the flights are discussed below.

Bernstein *et al*. (1997) developed a cyclone sector mapping guide that relates location for anywhere in North America with respect to synoptic system structure. Figure 7 is an example of the guide. LL used this guide for each forecast discussion to illustrate the target area with respect to the projected synoptic situation. The guide numbers the areas to reflect spatial distances ahead of, behind, within, or along the synoptic features: low pressure center, occluded low pressure center, warm front, occluded front, cold front, and Arctic front. For instance, one mission was in area 10 (occluded low) while another was in area 48 (ahead of a warm front away from the parent low). Each area has an inherent climatology related to icing potential that can now be sampled with dual pol radars across the U.S. possibly leading to association with dual pol radar features.

To gain an appreciation of the flight planning, an overview of the 2013 missions follows. Three icing missions were executed – on February 19, 26, and 28 – totaling 14 flight hours with 8 hours of weather probing in the target areas. Figure 8 shows the flight tracks for February 19 (black), 26 (red), and 28 (yellow). The optimal KBUF radar volume space is outlined with 25 km range rings (white) to 100 km (green). The area east of KBUF, especially over Lake Ontario, is restricted military air space not available for probing but it was open to transit. CWKR marks the King City radar location. NRC marks the Ottawa base. Concentrated swirls represent spiral probing through a deep layer. Areas of back and forth transects are evident as well. The flight altitudes ranged from a few thousand feet up to cloud top around 20 - 25 thousand feet.

An operational rhythm was established by February 13th for (usually) twice daily weather briefings led by LL that continued through March 4. Each briefing included discussion of the synoptic situation anticipated for the following five days with a yes-no-maybe verdict regarding worthiness for an icing mission. A briefing document was provided that included a marked-up cyclone sector mapping guide. For a 'go' mission verdict, LL also produced a flight plan document that included a target box in the KBUF radar range. This was updated about one hour prior to leaving home base at the Ottawa International Airport (NRC on Figure 8). Besides the usual weather forecasting challenges, LL had to also account for timing uncertainty regarding leaving the Ottawa base due to considerations for deicing, crew availability, and time of day. The time of day issue was resolved part way through the campaign when all pilots were night flight certified. Once a flight was certain for the next day, LL notified KBUF and KCLE radar operators to make a special request to scan with VCP12 or 212 (most frequent updating scanning). For the February 28 icing mission, LL suggested the radars be operated as they normally would for the given situation. This was suggested because realistically this is what dual pol algorithms would have available to process without special LL requests. The operators used clear air mode VCP31 that exhibits more sensitivity but updates every 10 minutes (6 minutes longer to update than VCP12 or 212). Lastly, LL notified the Cleveland ARTCC who supported the missions by making extra effort to request pilot reports of icing.

Experience gained from the February 2012 icing mission put the focus on communication between LL guidance from the ground and the

Convair 580 for the 2013 missions. LL needed reliable real-time Convair position data. The Convair scientists and pilots needed real-time KBUF data with a marking of the Convair position. All needed real-time communication for live flight guidance (for where to transect or spiral as the weather evolved). By the final flight all criteria were worked out sufficiently to have an invigorating experience. Prior to that, communication via a satellite link on the plane was occasionally sporadic. This link was the lifeline for real-time guidance via a chat mechanism, position data, and for real-time KBUF and KCLE (Cleveland) radar data on the plane. The latter used LL's ftp server for access to the imagery. Gibson Ridge GR3 software was used to create images of NEXRAD Level 3 products augmented with the plane position and/or proposed transects. With communications established with the plane, the crew had access to KBUF (and KCLE) data through 3.5^{o} elevation angle scans of reflectivity, differential reflectivity, and hydrometeor classification.

5.2 Feb. 24, 2012: Cleveland NEXRAD – Verify Category B Ice Crystals

The first, collaborative icing mission of LL and NRC occurred on February 24, 2012 as an added leg to a longer mission NRC was executing. The features of interest were light snow showers moving across Lake Erie presenting Category B dual pol radar returns. Figure 9 depicts transects and spirals taken during the icing mission. Figure 10 highlights a key finding from this mission as shown with a strip of the particle imaging probe and KCLE hydrometeor classification, differential reflectivity (ZDR), and reflectivity (Z) products.

A white cross represents the Convair position within the KCLE radar's 0.9° and 1.3° elevation angle PPIs at 101 km range along azimuth 24° at around 2054 UTC. The plane altitude is about 2590 m (T = -15° C). The Category B, pseudo-ephemeral radar presentation is apparent: moderate positive ZDR (3 – 5 dB) with low Z (0 – 5 dBZ) along the edge or top of precipitation. The NEXRAD HCA depicts a broad area of dry snow (light blue) edged by ice crystals (pink). The imaging probe strip shows pristine dendrites in this area lacking evidence of riming backed up by the liquid water content (LWC) sensor reporting nil.

5.3 Feb. 19, 2013: Buffalo NEXRAD – Presence of Mixed Phase in Dry Snow Classified Area

All in situ data referenced in discussion of the 2013 icing missions is preliminary and remains to be finalized (quality controlled).

The icing mission on February 19, 2013 featured precipitation ahead of a warm front followed by a cold front. The precipitation and cloud ahead of the warm front and along the cold front are known to be regions favorable for potential icing hazards. In Figure 11 the flight track (black) is overlaid on the 0.5° elevation angle PPI depicting HCA's hydrometeor classification. The Convair position is within the KBUF radar's PPI at 46 km range along azimuth 1° at around 1404 UTC. This is basically due north of KBUF on the south shore of Lake Ontario. The plane altitude is about 1740 m (T = -3° C). Commonly, LL has observed HCA to show a very broad dry snow (DS, blue) classification in this and many other situations but suspects there are at least pockets of mixed phase that could pose an icing hazard. Microphysically, dry snow does not exclude the presence of supercooled water.

Figure 12 shows time series plots of Liquid Water Content (LWC) and temperature measurements for the entire flight, and examples covering 14:10 – 14:40 UTC of radar reflectivity vertical cross-sections measured by the NRC Airborne W-band radar, and PMS 2D-C particle image data. The airborne W and X band radar data show a well defined melting layer for the first half of the flight at about one kilometer altitude with cloud tops reaching 6 km. The aircraft stayed above the melting layer and sampled mixed phase, super cooled, and glaciated clouds in a temperature range of -28° C to -4° C. As shown in the example period of Figure 12, the maximum LWC of 0.4 g m^{-3} was measured just above the melting layer at a temperature of about -5° C.

This mission focused on probing the vast dry snow classification region shown in Figure 11. However, as shown in Figure 12, liquid water was observed during non-trivial portions along the flight track in the dry snow classification region. The image strips show a mix of crystals types (irregular shapes, aggregates, needles). The crystals appear dense compared to the fine structure found during the Lake Erie mission. This is consistent with the crystal habit for warmer temperatures (Figures 1 and 2). Based on the crystal habit, water supersaturation is likely. LL will explore some methods to determine if the HCA has current information in the underlying processing that could be used to indicate the mixed phase or has a potential to incorporate a new mixed phase class.

5.4 Feb. 26, 2013: Buffalo NEXRAD – Moderate to Severe Clear Icing

The icing mission the night of February 26, 2013 is notable for the Cleveland ARTCC issuing a significant weather alert for moderate to severe clear icing conditions south of KBUF. As seen in the representative reflectivity image (upper left, Figure 13), the flight track (red) includes transects and spirals within the alert area west and south of the radar.

Figure 14, as in Figure 12, shows time series of LWC and temperature with example (00:55 – 01:50 UTC) radar reflectivity vertical cross-sections measured by the NRC W-band radar and samples of PMS 2D-C imagery. The aircraft sampled clouds with a temperature range of ~-27° C to +1° C. Supercooled drops were observed at temperatures as cold as -27° C with a maximum LWC of 0.35 g m^{-3} observed at a temperature of -10° C. The particle imagery shows diverse particle compositions (rain, melting crystals, large aggregates, needles, and irregular shape particles of various sizes). The NAWX radar vertical cross-sections show a well defined melting layer between altitudes of 1.5 – 2.2 km with a maximum reflectivity of over 55 dBZ with cloud tops exceeding 10 km in a part of the flight segment. Unlike the February 19 flight, the aircraft briefly descended below the melting layer. Figure 14 shows the vertical radar cross-section and examples of 2D-C particle images as the aircraft ascended from temperatures of +1^{o} C to -10^{o} C.

The Convair position is within the KBUF radar's PPI at 56 km range along azimuth 261° at around 0050 UTC. This is at the red swirl on the north shoreline of Lake Erie just past the 50 km range as seen in Figure 8. The plane altitude is about 1360 m (T = +2.5° C). Reflectivity values to at least 57 dBZ were observed at the time from KBUF. Differential reflectivity for that region shows positive values from 2 – 4 dB that are consistent with medium-large sized drops. The particle image strip in Figure 13 verifies the presence of drops. Temperatures in this region as probed by the Convair were within a few degrees Celsius of freezing. At the time of the image strips in Figure 13, the Convair was in greater than 0° C air but at lower altitudes the air was below freezing. So, medium-large drops were falling through multiple freezing levels.

The hydrometeor classifications from the NEXRAD HCA are incredibly diverse indicative of a dynamic environment but possibly also because it cannot handle multiple freezing level crossings. Virtually every class except clutter classes (BI – biologicals; GC – ground clutter) are represented: IC – ice crystals; DS – dry snow; WS – wet snow; RA – light rain; HR – heavy rain; BD – big drops; GR – graupel; HA – rain/hail. This case will require careful examination of the particle imaging and liquid water content (LWC) data. The pilot related to the LL mission scientist that these situations with larger supercooled drops and clear ice are a particularly dangerous icing hazard if an aircraft is not prepared to handle it. The liquid water spreads across the wings as it freezes, altering the aerodynamics. Supercooled water in cloud droplet form freezes on contact.

5.5 Feb. 28, 2013: Buffalo NEXRAD – Hexagonal Plates

The icing mission of February 28, 2013 will be remembered for the considerable observations of hexagonal plate crystals. As seen in the representative reflectivity image (upper left, Figure

15), the flight track (yellow) includes transects and spirals around the radar. The Convair position is within the KBUF radar's PPI at 33 km range along azimuth 296° at around 1908 UTC. This is at the concentration of yellow transects along the Niagara Frontier just past 25 km as seen in Figure 8. The plane altitude is about 1170 m (T = -6.6° C).

Figure 16 shows similar plots as Figures 12 and 14, but for the February 28 flight. The aircraft sampled diverse conditions ranging from glaciated clouds, mixed phase, and super cooled cloud volumes at temperatures in a range of -30^o C to -5^o C. The maximum observed LWC range from 0.15 g m^{-3} to 0.8 g m^{-3} at a temperature of -10^o C. The near field (~100 m range) of NAWX radar reflectivity shows reflectivity of less than -15 dBZ in all liquid cloud volumes and generally > 0 dBZ in the clouds with all ice crystals. The crystals sampled range from small irregular crystals to pristine plates to aggregates. There is a flight segment where the dominant crystals were mainly pristine plates. Williams *et al*. (2013) discuss this icing mission including the segment where the aircraft sampled extensive cloud volumes dominated by pristine plates in detail. From the KBUF radar (Figure 15), note the weak returns much of it below 0 dBZ. KBUF was operating in VCP31 as it typically does for these situations and is better able to depict structure in the weaker returns. Coinciding with the weak reflectivity are high values of differential reflectivity. Positive values from 3 – 6 dB are observed along the edge of the precipitation (Category B). It is often considered that such radar returns should be from anisotropic flat crystals. Through on-demand, special vertical soundings in Indiana by Valparaiso University students and knowledge of the crystal habit diagram, LL has suspected the crystals in question are flat, hexagonal plates. International atmospheric science literature states such crystals rarely are observed in nature despite findings of such in cold chamber experiments. Notably, this icing mission made significant discovery of flat, hexagonal ice crystals. The particle imaging strips in Figure 15 bear out the presence of hexagonal form plates. Some of the mission scientists with many years' icing mission experience remarked never seeing anything remotely like this mission's finding. A LL hypothesis is that the synoptic situation favored a steady condition of supersaturation and temperature to yield widespread hexagonal plate ice crystals courtesy of a three-day-old occluded low pressure system. An objective of any future missions should be to probe a similar situation to further verify or refute the uniqueness of the discovery.

From an icing perspective, Figure 16 indicates intermittent supercooled LWC during intervals characterized by hexagonal flat plates. Further analysis to precisely analyze this mission is planned. Regarding hydrometeor classification (lower image of Figure 15), often times these regions of hexagonal plate ice crystals were classified as Unknown (UK, purple). It might be possible to expand the NEXRAD HCA IC (ice crystal) classification to include such situations as observed on this flight if LWC is deemed small or non-existent.

6. SUMMARY

The importance of in situ icing missions cannot be understated regarding the validation and verification of dual pol hydrometeor classifications and the presence of icing hazard threats. With four icing missions in February 2012 and 2013, LL and NRC have been able to observe a small sampling of conditions likely to occur routinely (excepting possibly hexagonal plates). Edges of precipitation areas were probed. Variable mixed phase regions were encountered. Medium to large drops in a varying temperature regime were monitored. And, the elusive hexagonal plates were identified.

The ZDR bright band feature (zone 4, Figure 5) was not encountered in any of the flights. This zone in particular is suspected to be a mixed phase icing potential area. Low altitude, re-supercooling areas (zone 1) also have not been probed. With flights limited to the Lake Erie and Ontario area, they are somewhat limited regionally and February-only flights have limited missions thus far to the core of winter. Nonetheless, the preliminary findings should have broad applicability regionally and seasonally. Of course, an expanded icing mission portfolio would be ideal.

From the FAA's perspective, to recoup benefit from the NEXRAD dual pol upgrade, the icing missions' findings must be parlayed into useful information. The main challenge is to appropriately improve upon or expand the capabilities of the hydrometeor classifier. Is it possible to refine the dry snow or ice crystal classes? Could robust, separate mixed phase or supercooled water classes be developed? Likewise, incremental improvements to the IHL are necessary. Some might come through improved HCA (refined or new classes or handling multiple melting layers); and still, others through development of new techniques to rule in or out the icing hazard potential. All of these items populate a to-do list that could greatly benefit from future icing missions.

7. ACKNOWLEDGEMENTS

A critical support to the in situ icing missions was the operation of the NEXRAD radars in requested scan strategies. Tim Crum (NEXRAD ROC, retired), Jeff Waldstreicher (NWS Eastern Region HQ), Bob Laplante (WFO Cleveland), and David Zaff (WFO Buffalo) were instrumental in ensuring requests were met.

MIT LL's program for NEXRAD Dual Pol Enhancements has involved multiple partners whose expertise and capabilities have significantly advanced the development process. The partners are the folks from Valparaiso University, the National Severe Storms Laboratory, the National Center for Atmospheric Research, the National Research Council of Canada, and Environment Canada.

The FAA's NEXRAD program led by Steve Kim, Tom Webster, and Bill Bumgarner has been crucial in their support of the in situ icing measurements. They have recognized the important role for validation and verification.

8. REFERENCES

Bailey, M. P. and J. Hallett, 2009: A comprehensive habit diagram for atmospheric ice crystals: Confirmation from the laboratory, AIRS II and other field studies. *J. Atmos. Sci.*, **66**, 2888-2899.

Bernstein, B. C., C. A. Wolff, and F. McDonough, 2007: An Inferred Climatology of Icing Conditions Aloft, Including Supercooled Large Drops. Part I: Canada and the Continental United States. *J. Appl. Meteor*., **46,** 1857–1878.

Bernstein, B. C., F. McDonough, M. K. Politovich, B. G. Brown, T. P. Ratvasky, D. R. Miller, C. A. Wolff, and G. Cunning, 2005: Current icing potential: Algorithm description and comparison with aircraft observations. *J. Appl. Meteor*., **44,** 969–986.

Bernstein, B. C., T. A. Omeron, F. McDonough, and M. K. Politovich, 1997: The relationship between aircraft icing and synoptic-scale weather conditions. *Wea. Forecasting*, **12**, 742–762.

Hallowell, R. G., M. F. Donovan, D. J. Smalley, and B. J. Bennett, 2013: Icing Hazard Detection with NEXRAD IHL. *Proc. American Meteorological Society's 36th International Radar Conference, Breckenridge, CO.*

Korolev. A. and I. P. Mazin, 2003: Supersaturation of water vapor in clouds. *J. Atmos. Sci*., **60**, 2957-2974.

Park, H., A.V. Ryzhkov, D.S. Zrnic, and K-E. Kim, 2009: The Hydrometeor Classification Algorithm for the Polarimetric WSR-88D: Description and Application to an MCS. *Wea. Forecasting*, **24**, 730–748.

Smalley, D. J., B. J. Bennett, M. F. Donovan, R. G. Hallowell, K. T. Hood, E. R. Williams, D. Zrnic, A. V. Ryzhkov, T. J. Schuur, H. D. Reeves, J. M. Krause, P. Zhang, M. Kumjian, J. Picca, S. Ganson, J. C. Hubbert, D. Albo, S. Ellis, M. Dixon, A. Weekley, M. Politovich, G. Cunning, C. Wolff, F. McDonough, T. Bals-Elsholz, R. Evaristo, and A. Stepanek, 2011: Multiple national laboratory and university partnership to develop dual polarization weather radar for the FAA. *Proc. American Meteorological Society's 27h Interactive Information Processing Systems Conference, Seattle, WA.*

Williams, E. R., D. J. Smalley, M. F. Donovan, R. G. Hallowell, K. T. Hood, B. J. Bennett, M. Wolde, M. Bastian, A. V. Korolev, 2013: Validation of NEXRAD radar differential reflectivity in snowstorms with airborne microphysical measurements: Evidence for hexagonal flat plate crystals. *Proc. American Meteorological Society's 36th International Radar Conference, Breckenridge, CO.*

Williams, E. R., D. J. Smalley, M. F. Donovan, R. G. Hallowell, K. T. Hood, B. J. Bennett, R. Evaristo, A. Stepanek, T. Bals-Elsholz, J. Cobb, and J. M. Ritzman, 2011: Dual polarization radar winter storm studies supporting development of NEXRAD-based aviation hazard products. *Proc. American Meteorological Society's 35th International Radar Conference, Pittsburgh, PA.*

Wolde, M., and G. Vali, 2001a: Polarimetric signatures from ice crystals observed at 95 GHz in winter clouds, Part I: Dependence of crystal form. *J. Atmos. Sci.*, **58**, 828-841.

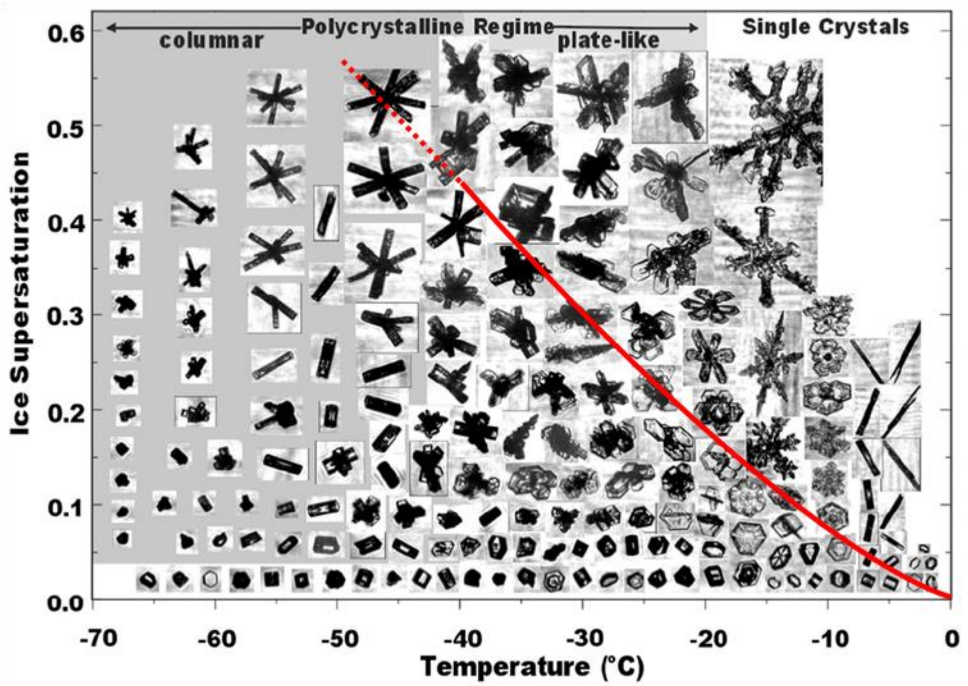

Figure 1. The detailed crystal habit diagram, with temperature and humidity dependence, from Bailey and Hallett (2009). The red line represents water saturation with sub- to the left and super- to the right. The entire diagram is ice saturated or supersaturated.

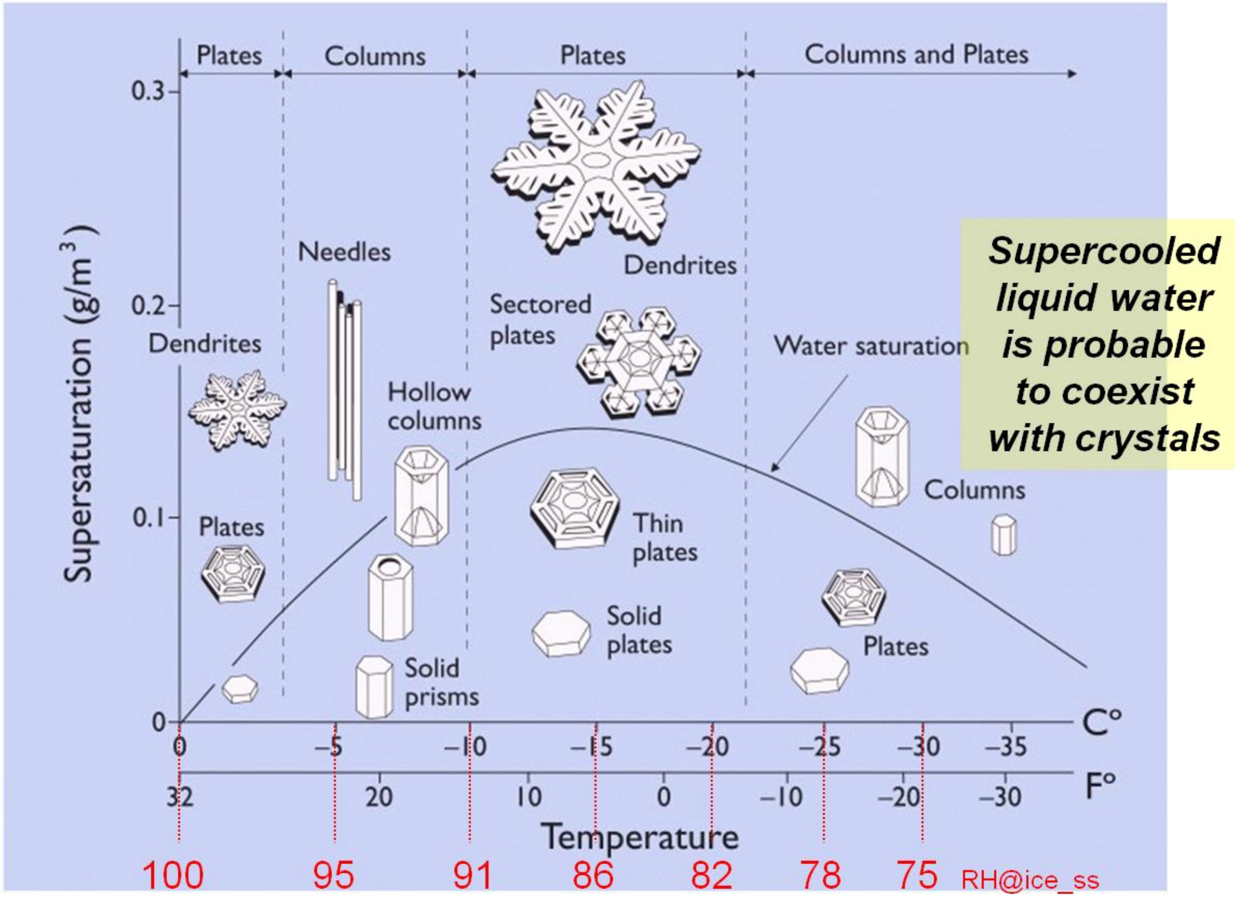

Figure 2. A summarization of Figure 1 with the arcing curve representing water saturation (sub below, super above). The red values are the relative humidity with respect to liquid water at ice saturation.

HCA Categories

- **GC** Ground clutter / anomalous propagation
- **BI** Biological
- **DS** Dry snow
- **WS** Wet snow
- **IC** Ice crystals
- **BD** Big drops
- **RA** Rain (light and moderate)
- **HR** Heavy rain
- **GR** Graupel
- **HA** Hail (mixed with rain)
- **UK** Unknown
- **ND** No data (less than threshold)

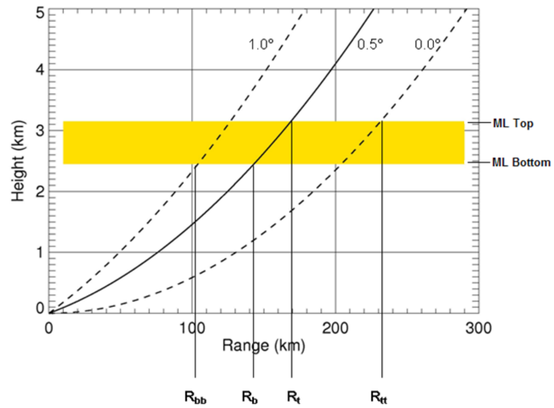

Melting Layer Constrains HCA

- **Completely below:**
  - **GC, BI, BD, RA, HR, HA, UK, ND**
- **Partly below:**
  - **GC, BI, WS, BD, RA, GR, HR, HA, UK, ND**
- **Mostly within:**
  - **GC, BI, DS, WS, BD, GR, HA, UK, ND**
- **Partly above:**
  - **GC, BI, DS, WS, IC, BD, GR, HA, UK, ND**
- **Completely above:**
  - **DS, IC, GR, HA, UK, ND**

Figure 3. The NEXRAD Hydrometeor Classification Algorithm scheme allows or restricts categories in reference to the location of a single melting layer. Five melting layer regions are considered. (Image courtesy Mike Istok, NWS).

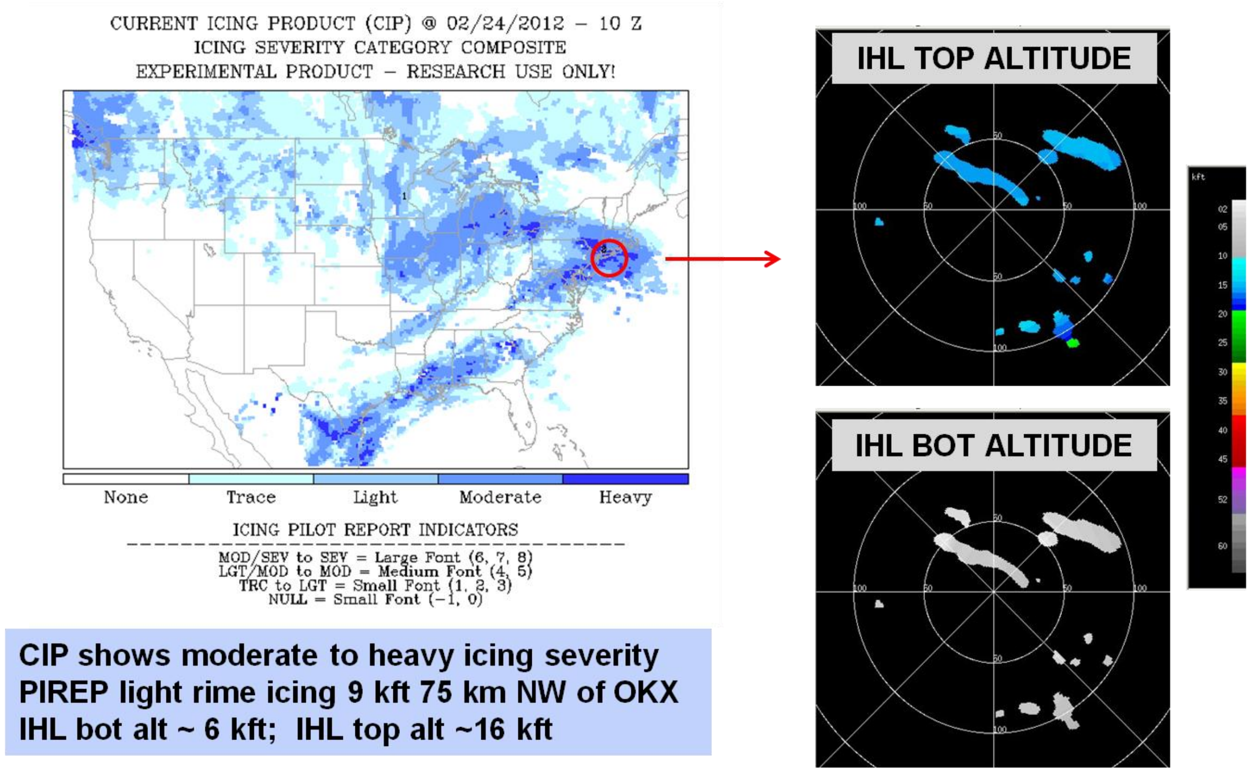

Figure 4. The Icing Hazard Levels (IHL) product consists of an altitude top (top) and altitude bottom (bot) based on the presence of the graupel hydrometeor classification within the individual elevation angle tilts of a radar volume. This example for the KOKX NEXRAD (Upton, NY) from Feb. 24, 2012 around 10 UTC shows good corroboration with icing pilot reports (PIREP) in the area as well as with the Aviation Weather Center's Current Icing Product for that time in that location.

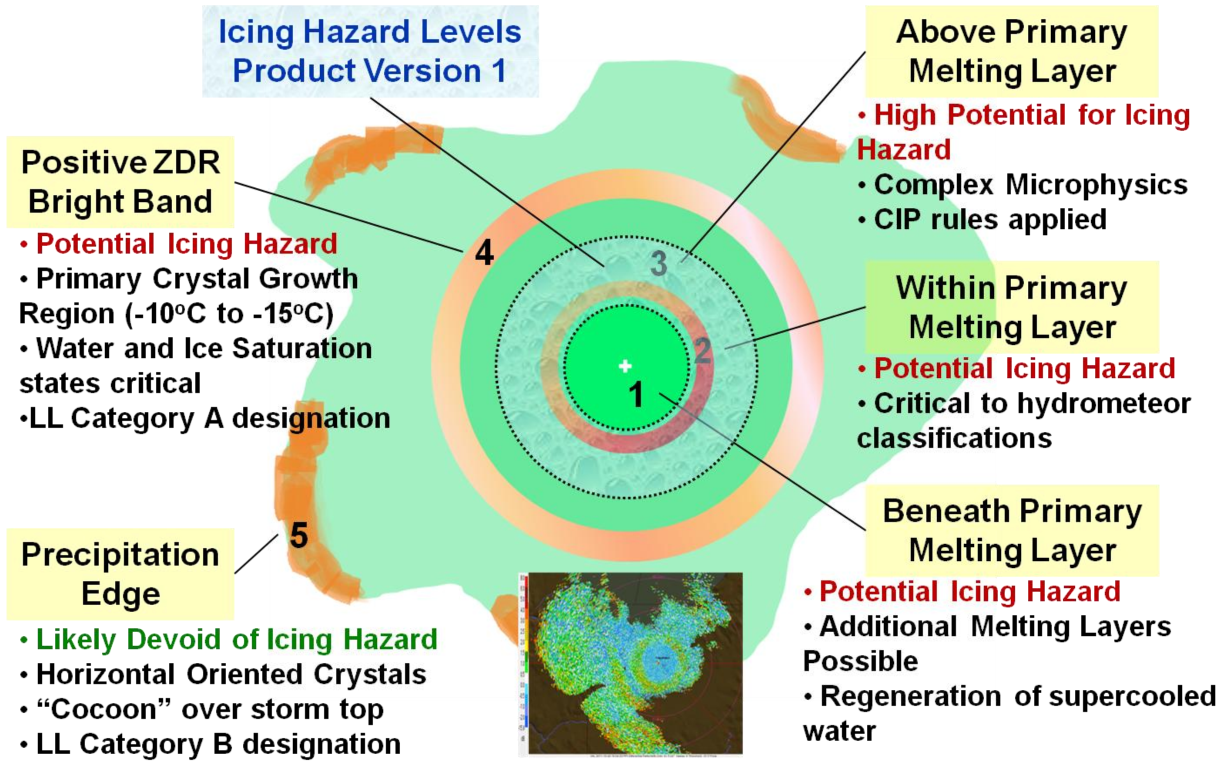

Figure 5. Regions of potential icing hazard are listed from a radar plan position indicator perspective (i.e. – elevation angle tilt). Some potential icing hazard regions yield somewhat familiar dual pol radar signatures. The Icing Hazard Levels product version 1 addresses portions of regions 2 and 3.

Figure 6. A collection of frozen hydrometeors collected during a late winter storm in eastern Massachusetts shows a variety of types. Graupel (ball-like), rimed dendrites, rimed aggregates, and rimed needles were collected. These ground based collections aid in interpretation of the dual pol signatures from aloft but in situ icing missions are preferred.

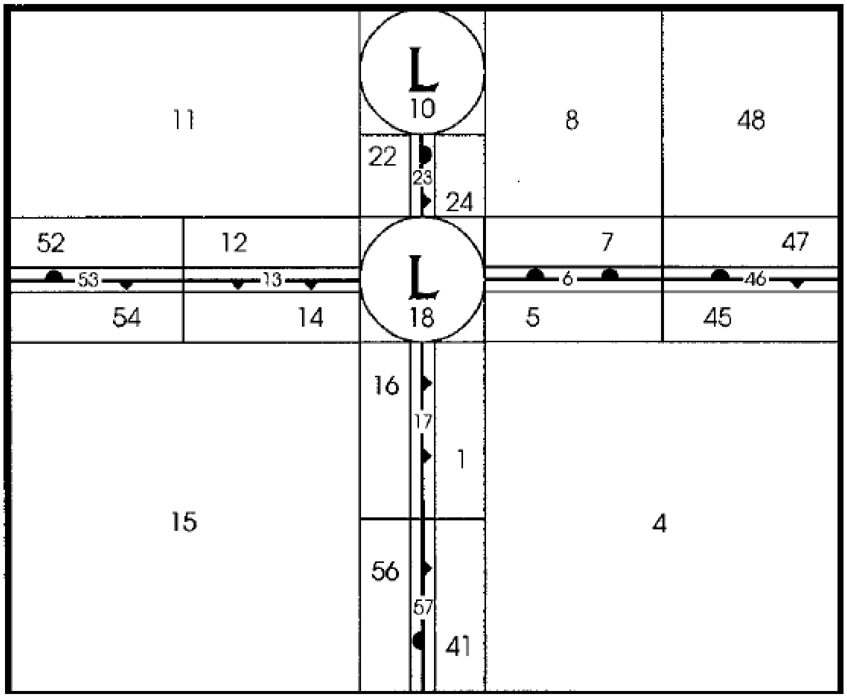

Figure 7. From Bernstein *et al*. (1997) Fig. 5(a), this diagram is a cyclone sector mapping guide. Numerical coding is assigned to each area as it relates in distance to standard synoptic features: low pressure (18), occluded low pressure (10), cold front (17), Arctic cold front (13), warm front (6), occluded front (23) and various types of stationary fronts (53, 46, 57). This guide was used to aid in situ icing mission forecasts.

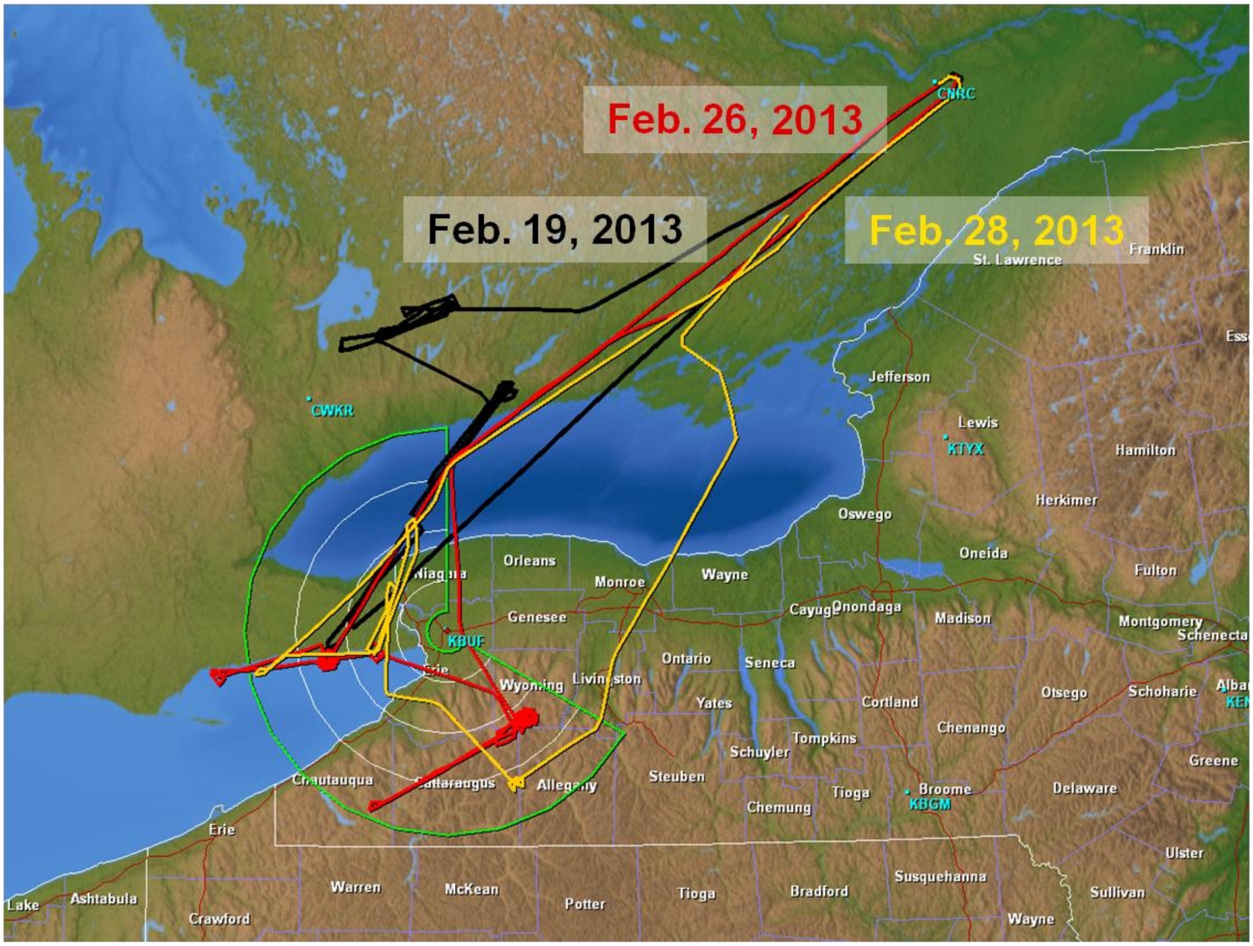

Figure 8. A summary of the 2013 icing mission flight tracks. NRC denotes the start/end point at the home base of Ottawa International Airport. CWKR is the King City dual pol C-band radar. KBUF is the dual pol S-band NEXRAD radar with 25 km range rings (white, green for 100 km). Highlights of the mission findings are discussed in the text.

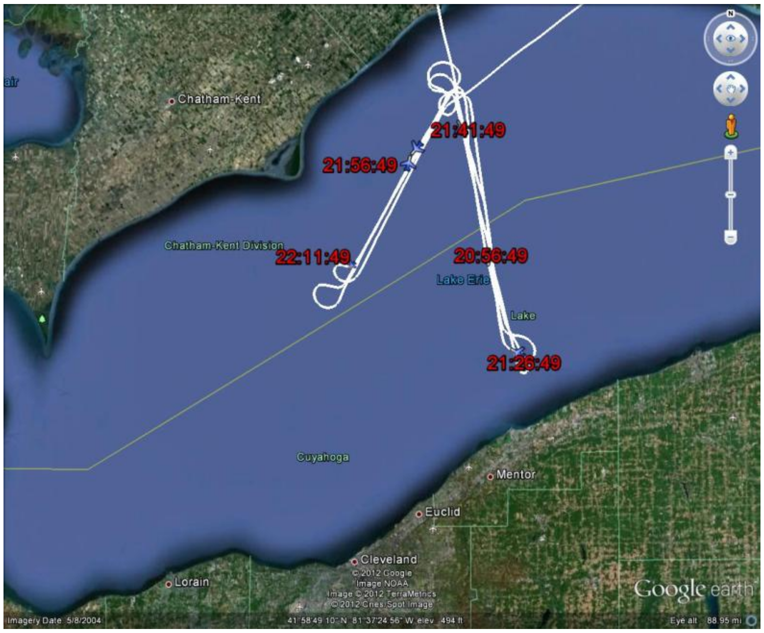

Figure 9. The icing mission flight track is shown over Lake Erie from Feb. 24, 2012 within radar range of the KCLE dual pol NEXRAD. Swirls represent spiral sweeps over a range of altitudes.

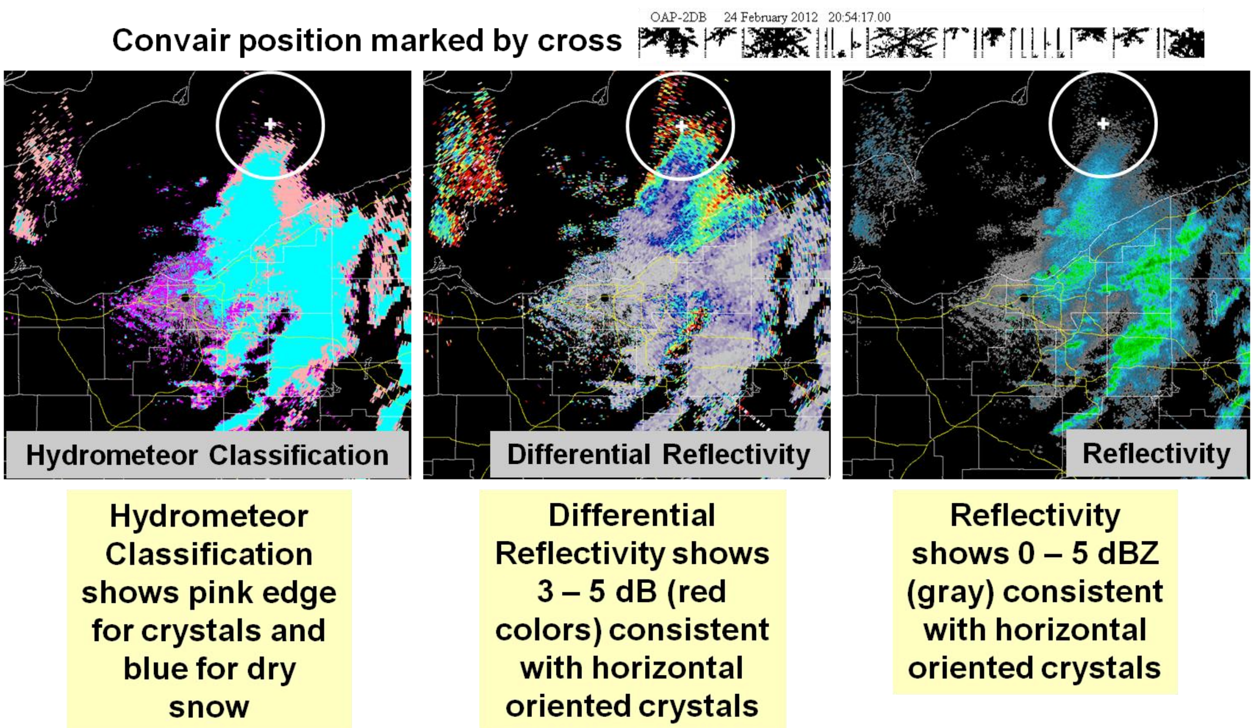

Figure 10. Representative results from the KCLE dual pol NEXRAD are presented for hydrometeor classification (pink, ice crystals) from the NEXRAD HCA, differential reflectivity (high values), and reflectivity (low values) with a white cross to mark the Convair 580's position. This Category B type case is consistent with the observed values and verified by the in situ icing mission particle probe imagery showing dendrites (sample image upper right).

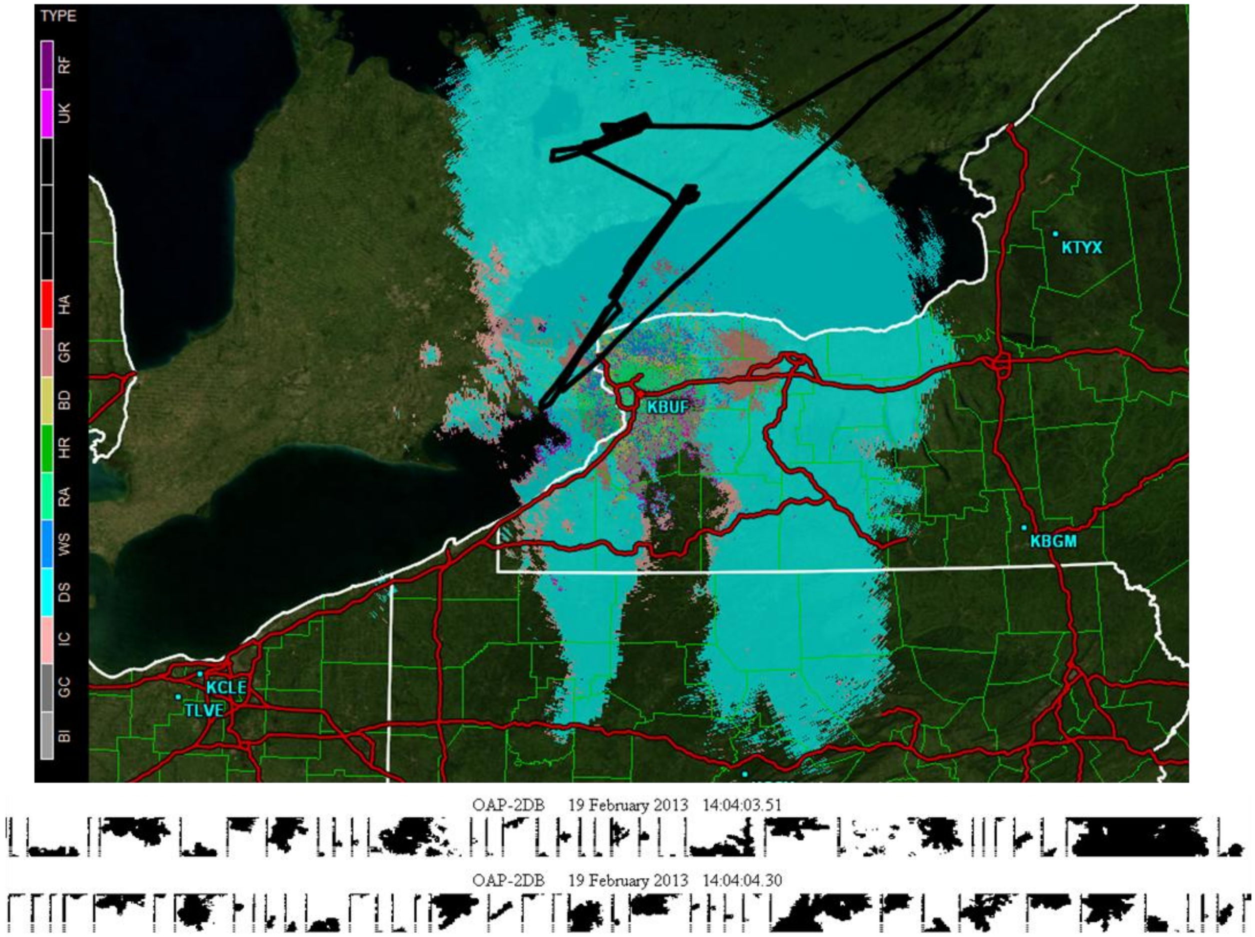

Figure 11. The icing mission flight track (black) is shown over Lake Ontario and Canada from Feb. 19, 2013 within radar range of the KBUF dual pol NEXRAD overlaid on NEXRAD HCA hydrometeor classification. Swirls represent spiral sweeps over a range of altitudes. Sample particle probe imagery for 1404 UTC is shown.

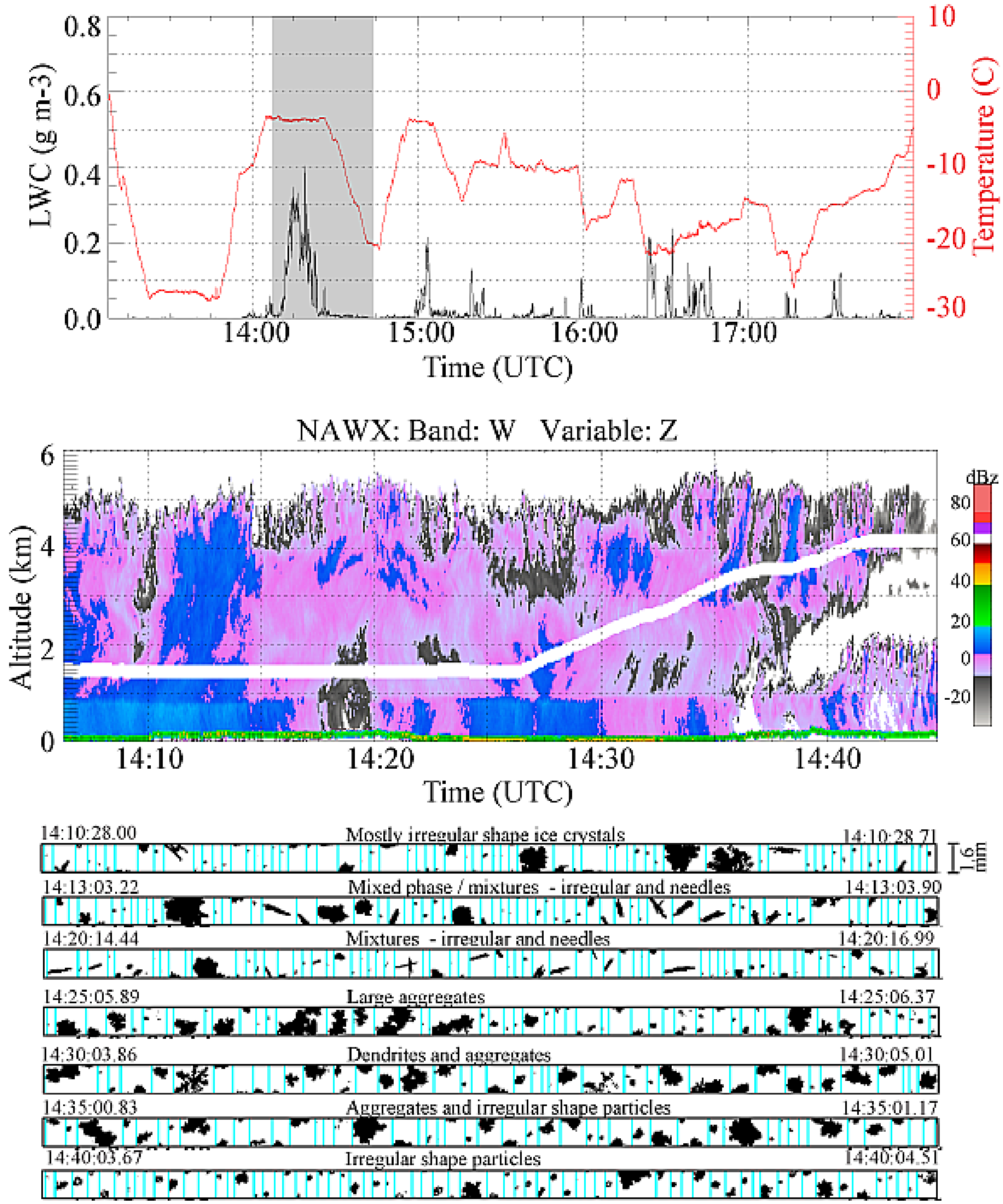

Figure 12. Top: Time series plots of Liquid Water Content (LWC) and Temperature measured during the NRC Convair 580 flight on February 19, 2013 from the operational base in Ottawa, Canada to areas within the KBUF radar range. Middle: Vertical profiles of reflectivity (Ze) measured by the NRC Airborne W-band radar corresponding to the shaded segments in the time series plot. The white line in the image shows the aircraft altitude. Bottom: Samples of particle images measured by a PMS 2D-C probe corresponding to the vertical radar cross-section.

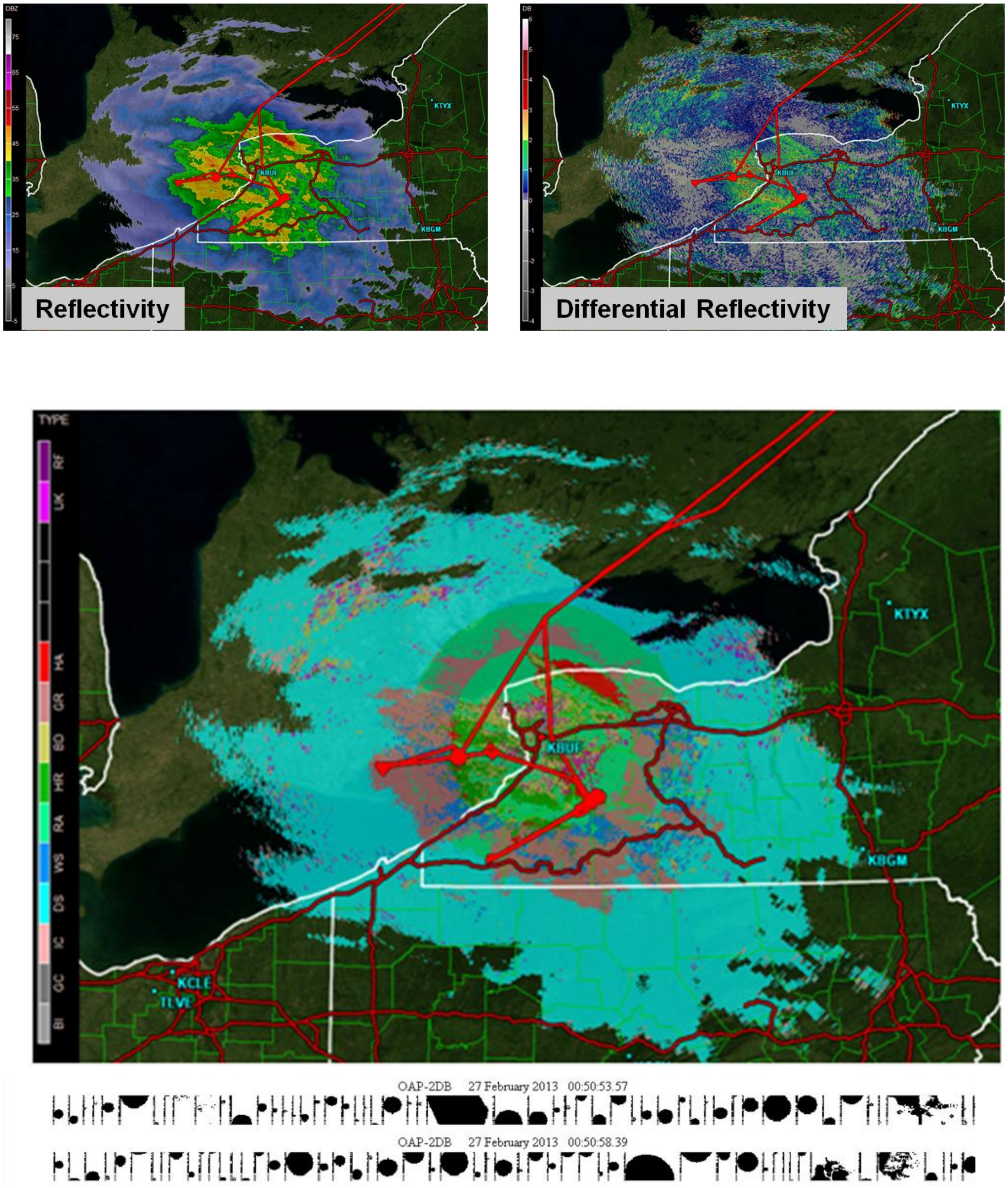

Figure 13. The icing mission flight track (red) is shown over Lake Ontario, Canada, and the U.S. from the evening of February 26, 2013 within radar range of the KBUF dual pol NEXRAD overlaid on NEXRAD HCA hydrometeor classification. Swirls represent spiral sweeps over a range of altitudes. Sample particle probe imagery for 0050 UTC (February 27, 2013) is shown.

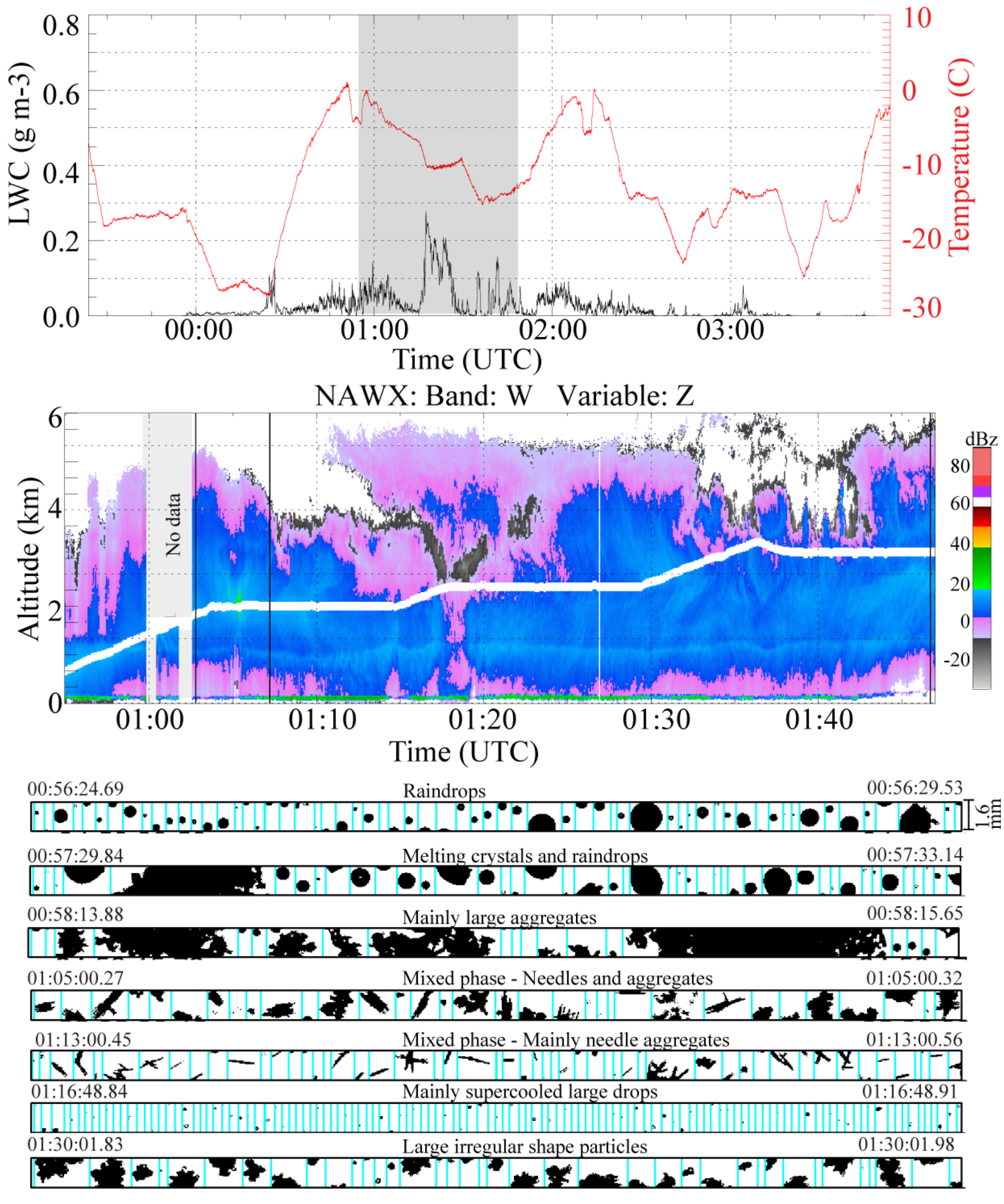

Figure 14. Same as in Figure 12 except for the February 26, 2013 NRC Convair 580 flight (February 27, 2013 UTC times).

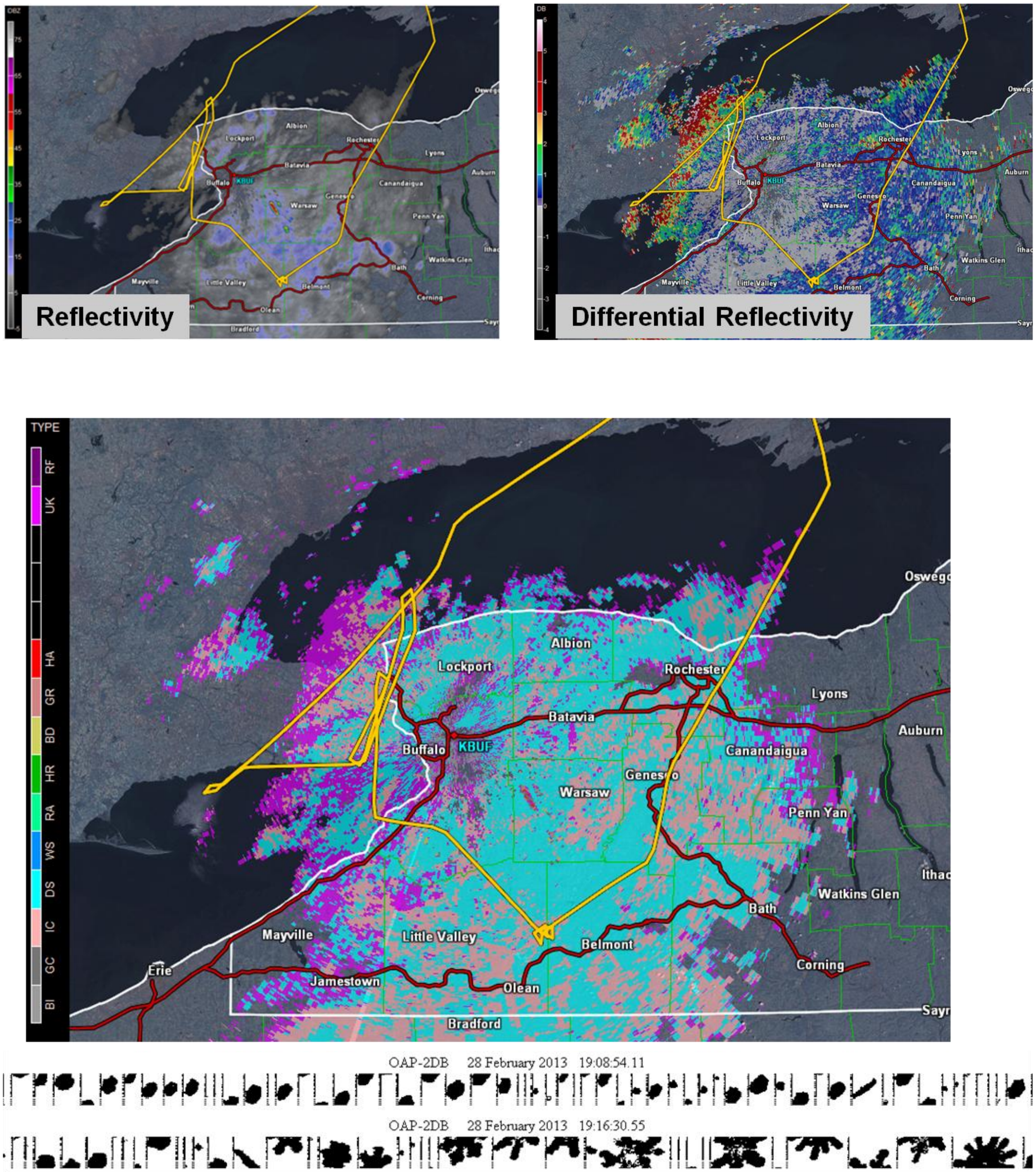

Figure 15. The icing mission flight track (yellow) is shown over Lake Ontario and Canada from Feb. 28, 2013 within radar range of the KBUF dual pol NEXRAD overlaid on NEXRAD HCA hydrometeor classification. Swirls represent spiral sweeps over a range of altitudes. Sample particle probe imagery for 1908 UTC is shown.

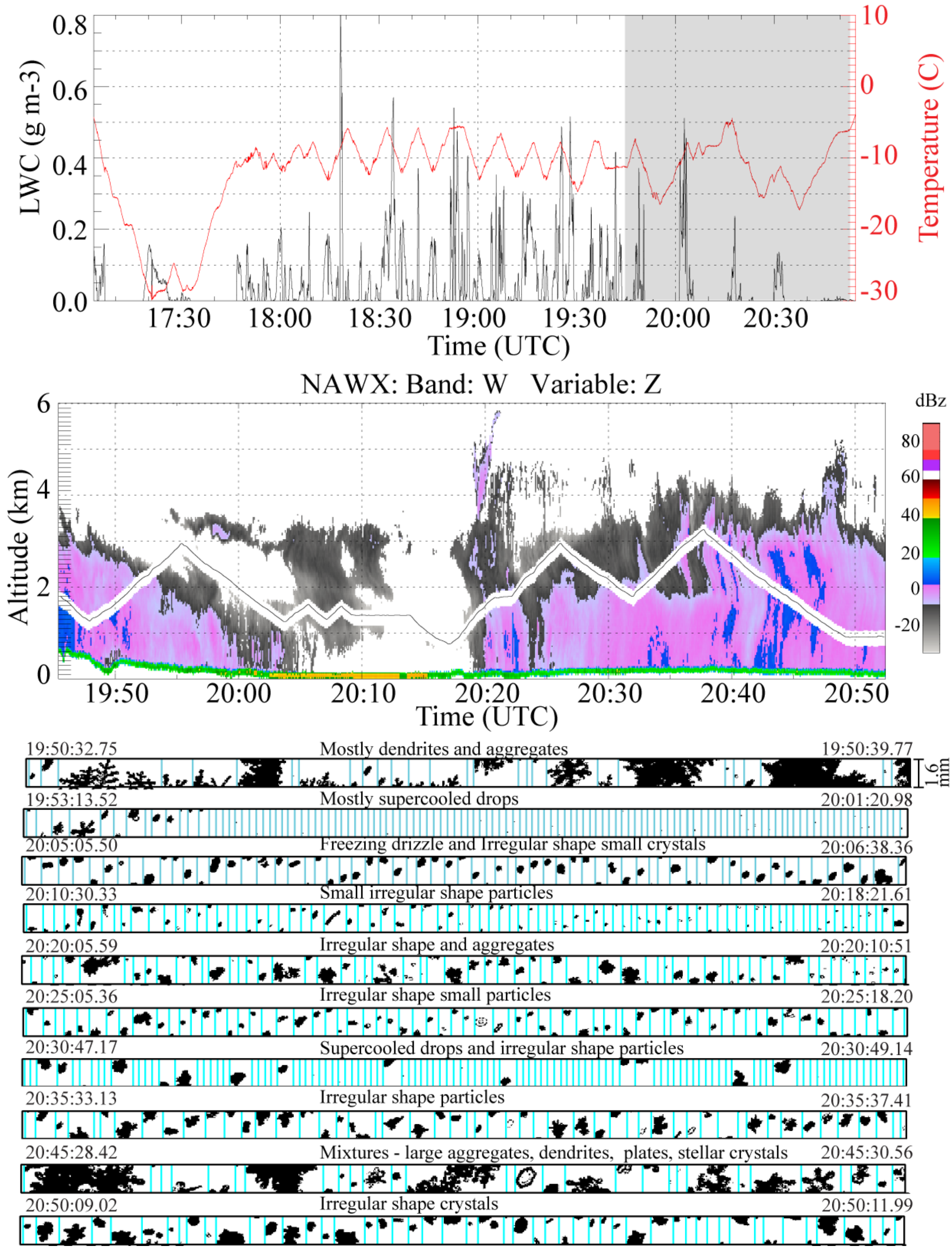

Figure 16. Same as Figure 12 except for the February 28, 2013 NRC Convair 580 flight.